

Pulse compression waveforms design and Cross-ambiguity processing for Radar applications

Touati Nadjah
and Tatkeu Charles
IFSTTAR

Villeneuve d'Ascq 59650, France

Email:

nadjah.touati@ifsttar.fr
charles.tatkeu@ifsttar.fr

Rivenq Atika
and El hillali Yassin
Université de Valenciennes
IEMN-DOAE

Email:

atika.menhaj@univ-valenciennes.fr
yassin.elhillali@univ-valenciennes.fr

Chonavel Thierry
Télécom Bretagne
UMR CNRS 6285 Lab-STICC
Brest 29200, France
Email:

thierry.chonavel@telecom-bretagne.eu

Abstract—Radar waveforms design is an important step to design a whole radar system. In this paper, several waveforms based on modified Costas codes are used. The properties and performances are tested and compared. We propose a detection based on cross-ambiguity calculation for these waveforms. Indeed, such a processing is interesting when delay and Doppler should be estimated. The performances are evaluated in several scenarios in presence of noise and multiple targets. The waveforms are also tested on real experimentation hardware.

Keywords—Radar waveforms, Costas signals, Auto-ambiguity function, Cross-ambiguity function, matched filter.

I. INTRODUCTION

In radar applications, high range resolution may be obtained with short pulses and hence large bandwidths. However, short pulse radars shows limitations due to the high peak power required to achieve the large pulse energy. On the other hand, a long pulse can have the same bandwidth (resolution) as a short pulse if it is modulated in frequency or phase. Pulse compression is a technique that allows a radar to simultaneously achieve the energy of a long pulse and the resolution of a short pulse by modulating the pulse [1]. Two most important classes of pulse compression waveforms are frequency modulated signals and phase coded signals [2]. Costas codes are a sort of frequency hopping codes that achieve the thumbtack auto-ambiguity function AAF needed in radar applications [3] thanks to their optimized frequency evolution.

In this paper, waveforms based on modified Costas signals are synthesized. These waveforms offers flexibility to Costas codes by introducing pulse diversity. More specifically, the modification consists in widening the frequency spacing between Costas frequency hops and replacing constant frequency pulses by other pulse compression waveforms. A detection using cross-ambiguity function CAF calculation is operated for proposed signals. Performances are tested in a Radar scenario considering noise and single/multiple target context. The tests of the waveforms on real experimentation Hardware are also shown.

The paper is organized as follows: in section II, the principle and properties of used waveforms, in this work, are discussed. In section III, the principal of target detection using cross-ambiguity calculation is exposed and applied for the

above signals in presence of noise and/or multiple targets. Finally in section IV, some real experimentation results are shown.

II. WAVEFORM DESIGN

In this part, we will discuss pulse compression waveforms used in this work. Indeed, we use waveforms based on modified Costas codes. The modification consists in widening frequency separation between Costas frequency hops and replace constant frequency pulses with other waveforms.

a) Standard Costas signals: A Costas signal consists in an $M \times M$ time-frequency code with a randomlike ordering $[a_1 a_2 \dots a_M]$. Each frequency pulse consists in a constant frequency signal of duration t_p . The frequency hopping Δf is at least equal to the inverse of pulse duration, $\Delta f = \frac{1}{t_p}$. This condition forces the AAF to have a single centered mainlobe and low sidelobes at all other points. This condition imposes a gradual scan of the bandwidth by a $\frac{1}{t_p}$ step. Hence, it is sometimes interesting to increase the frequency spacing beyond this condition that is setting $\Delta f > \frac{1}{t_p}$. However, increasing the frequency spacing while keeping constant frequency pulses is not convenient. Indeed, when orthogonality condition is not satisfied, grating lobes around the main temporal lobe of the autocorrelation function ACF of the signal will appear. Based upon previous considerations, a change in Costas pulse waveforms is operated in order to allow the lowering of grating lobes. Depending on pulse waveform nature, several modified signals exists:

b) Costas-LFM signals: Modified Costas signals where proposed when $(\Delta f > \frac{1}{t_p})$, in [4]. They consists in replacing constant frequency pulses by Linear Frequency Modulated LFM ones. This approach involves placing nulls of single LFM ACF exactly where the grating lobes are located, and thus removes them completely. This takes place under the restrictions of an appropriate choice of the LFM bandwidth B_p according to Costas frequency spacing.

c) Phase coded Costas signals: Another way to modify Costas codes consists in introducing phase coding in Costas pulses[5]. When used phase codes show good autocorrelation properties grating lobes are lowered significantly. Furthermore, to avoid several periods of the signal to fall in the mainlobe the

TABLE I. MODIFIED COSTAS SIGNALS FOR A COSTAS SIZE $M = 8$ AND A TOTAL BANDWIDTH $B \approx 500\text{MHz}$

	Standard Costas	Costas-LFM	Costas-Hequi	Costas-P4	Doubly coded Costas
Main Costas size	8	8	8	8	8
$(t_p\Delta f, t_pB_p)$	(1,0)	(6,14.5)	(6,8)	(6,9)	(6,14.4)
$t_p(ns)$	16	113	100	102	112.8
$\Delta f(MHz)$	62.5	53.1	60	58.8	53.2
$B(MHz)$	500	500	500	500	500
$T(ns)$	128	904	800	816	902

phase code length must be at least equal to the novel spacing i.e. $L \geq t_p\Delta f$

d) *Doubly coded Costas signals*: The doubly coded Costas signals principle consists in using other Costas codes to encode the principal Costas pulses[6]. Indeed, under some conditions on secondary Costas parameters: size N , sub-pulse duration t_s and frequency spacing Δf_s , such a double Costas coding approach can be efficient in eliminating grating lobes. Indeed, the bandwidth of the secondary Costas $B_p = N \times \Delta f_s$ must be at least to the novel spacing i.e. $N^2 \times t_s \Delta f_s \geq t_b \Delta f$.

Previous described in are synththesised for a fixed bandwidth $B = 500\text{MHz}$. For modified Costas codes, we must select the pair of compatible $(t_p\Delta f, t_pB_p)$ according to conditions stated in [4], [5] and [6]. The overall bandwidth of the modified Costas signals is approximatively: $B_{\text{modified Costas}} \approx (M - 1)\Delta f + B_p$ instead of classical Costas signals bandwidth $B_{\text{classical Costas}} \approx M\Delta f = \frac{M}{t_p}$. This allow a better flexibility to achieve the needed bandwidth. Indeed, we fix the main Costas code [1, 3, 6, 7, 5, 4, 8, 2] of size $M = 8$ and calculate the pulse duration t_p , frequency spacing Δf according to the novel $t_p\Delta f$ product, and the overall signal duration T in each case. Results are shown in Table I, where an LFM chirp, a P4 phase code, a spectrally balanced Hadamard code and a Costas code are used to encode the main Costas pulses.

The auto-ambiguity function AAF represents the time response of a filter matched to given finite energy signal when the signal is received with a delay τ and a Doppler shift ν relative to the nominal values (zeros) expected by the filter [2]. The AAF is expressed by:

$$|\chi_{u,u}(\tau, \nu)| = \left| \int_{-\infty}^{+\infty} u(t)u^*(t + \tau)e^{j2\pi\nu t} dt \right| \quad (1)$$

where u is the complex envelope of the signal. This function allow evaluating performances of Radar waveforms. The ideal one consists in one centered spike and zeros elsewhere. ACF's of signals of previous signals are free of grating lobes thanks to valid combinations between main Costas parameters and pulse waveforms parameters as shown in reference works. The AAF's also result in centered spike and low sidelobes distributed in the delay-Doppler plan. The spike have a temporal width of $1/B$ and Doppler width of $1/T$. We note that modified signals show low sidelobes compared to standard Costas signals especially in the vicinity of the main lobe. However, in a real-life scenario, the received signal is the sum of multiple echoes delayed and Doppler shifted, corrupted by noise. The cross-ambiguity function CAF must be considered to find the spikes that will be centered in the true delays and Doppler shifts.

III. CROSS-AMBIGUITY FUNCTION

When a signal $u(t)$ is transmitted. The received echo signal will be the sum of several echoes corrupted by noise. It can be expressed by: $r(t) = \sum_{i=1}^K \alpha_i u(t - \tau_i) e^{j2\pi\nu_i(t - \tau_i)} + n_0(t)$, where $n_0(t)$ is an additive noise and (τ_i, ν_i) are delay and Doppler of the i^{th} target. The CAF $|\chi_{u,v}(\tau, \nu)|$ between the reference signal and the received echo, will be the sum of individual AF's centered in the true delay and Doppler shifts:

$$\chi_{u,r}(\tau, \nu) = \sum_{i=1}^K \alpha_i \chi_{u,u}(\tau - \tau_i, \nu - \nu_i) e^{-j2\pi\nu_i(\tau - \tau_i)} + n_1(t) \quad (2)$$

where $n_1(t)$ is the noise at the output of the cross-ambiguity function. In this section, we will present the application of the cross-ambiguity function CAF in a radar context. We will introduce the parameters of a radar into the CAF and display it. The purpose of this is two-fold: display performances of previous signals in presence of noise and multiple targets. The principle of calculation is presented in Fig 1.

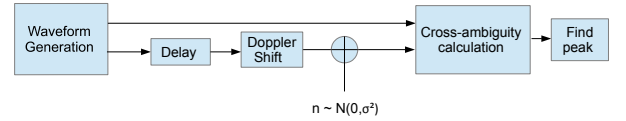


Fig. 1. Cross-ambiguity function CAF calculation principle between the reference signal and a noisy, time-delayed, frequency-shifted version

a) *CAF in noisy environment*: In this part, we propose to evaluate CAF properties in presence of noise. We propose to vary the $SNR = -20, -10, 0$ and 10dB . Results are presented in Fig 2, Fig 3, Fig 4, Fig 5, Fig 6. The operational scenario constructed here is when the received signal is corrupted by a delay $\tau = 16\text{ns}$ and a Doppler $\nu = 62.5\text{MHz}$.

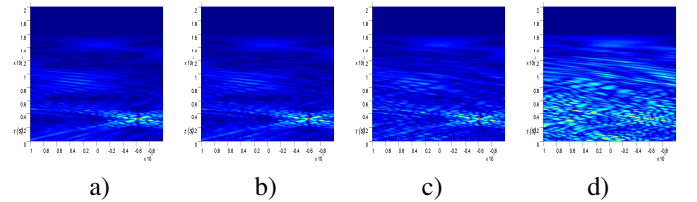


Fig. 2. CAF for a standard Costas signal: a) $SNR=10\text{dB}$, b) $SNR=0\text{dB}$, c) $SNR=-10\text{dB}$, d) $SNR=-20\text{dB}$

We can see that the CAF is almost transparent to the noise effect for SNR higher than -10dB . This is justified by the matched filter since it is the optimal linear filter for maximizing the SNR in the presence of additive noise. The effect start to

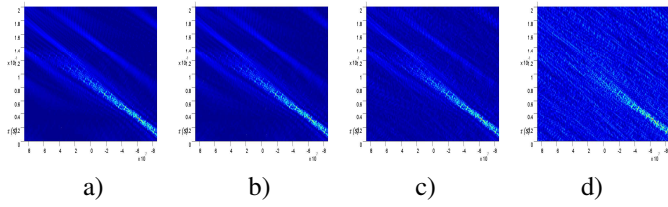


Fig. 3. CAF for a Costas-LFM signal: a) SNR=10dB, b) SNR=0dB, c) SNR=-10dB, d) SNR=-20dB

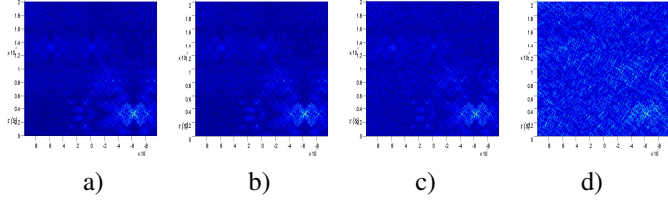


Fig. 4. CAF for a Costas-Hequi signal: a) SNR=10dB, b) SNR=0dB, c) SNR=-10dB, d) SNR=-20dB

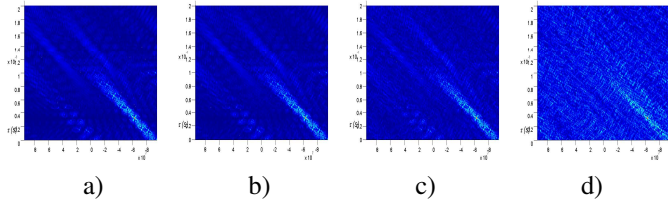


Fig. 5. CAF for a Costas-P4 signal: a) SNR=10dB, b) SNR=0dB, c) SNR=-10dB, d) SNR=-20dB

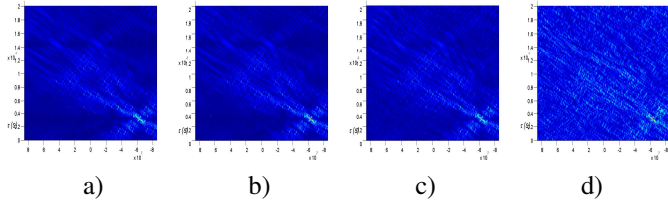


Fig. 6. CAF for a Doubly coded Costas signal: a) SNR=10dB, b) SNR=0dB, c) SNR=-10dB, d) SNR=-20dB

be felt for very lower SNR's, namely $-20dB$. We can see that the noise effect is more present in standard Costas signals than other signals since they already show higher sidelobes, and when corrupted by noise may increase and cause the appearance of spurious targets.

b) CAF in a multi-target scenario: In this part, the CAF is evaluated in the presence of several targets. Two notions are important in this case: Delay resolution and Doppler resolution. Delay resolution indicate the ability to resolve two targets with close delays. It depend on the bandwidth of the signals. The Doppler resolution indicate the ability to resolve two targets with close Dopplers. It depend mainly in the signal duration. We note that, in this case, the signals achieve the same delay resolution $\Delta\tau \approx \frac{1}{B} = 2ns$, but different Doppler resolutions depending on the signal duration of each signal: $\Delta\nu \approx \frac{1}{T}$. Two scenarios are considered depending in the position of targets in the CAF plan, in a noiseless context: 3 spaced targets and 3 close targets. Results for previous signals

are shown in Fig 7, Fig 8, Fig 9, Fig 10 and Fig 11.

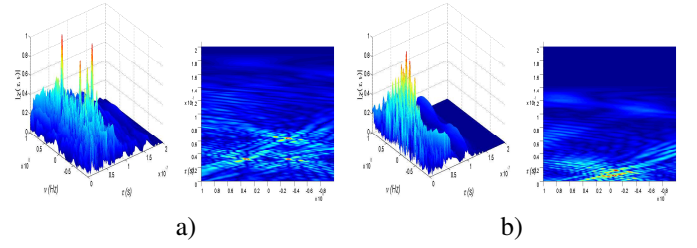


Fig. 7. CAF for a standard Costas signal: a) spaced targets scenario c) close targets scenario

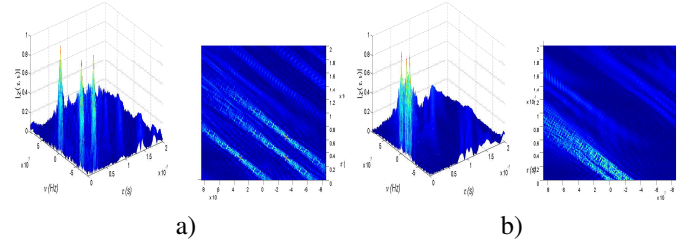


Fig. 8. CAF for a Costas-LFM signal: a) spaced targets scenario c) close targets scenario

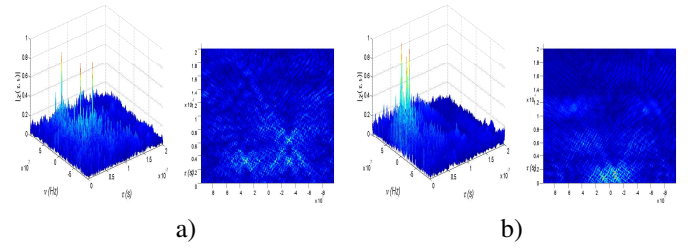


Fig. 9. CAF for a Costas-Hequi signal: a) spaced targets scenario c) close targets scenario

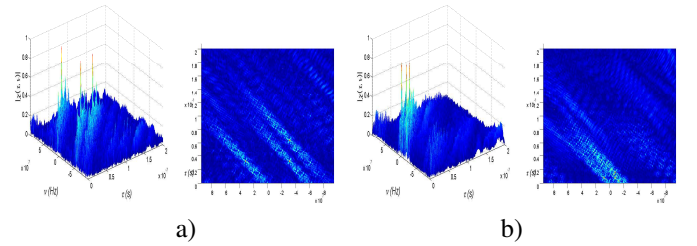


Fig. 10. CAF for a Costas-P4 signal: a) spaced targets scenario c) close targets scenario

The sidelobe level in the CAF plan is increased compared to a single target case. Indeed, since the CAF is the sum of individual CAF's, the sidelobe level increases when the number of targets increases. Especially in the vicinity of mainlobes (true target positions), high lobes may appear because of superposed sidelobes, and cause the appearance of spurious targets. Such a case appear in the closed targets scenario in the case of standard Costas signal shown in Fig 7. For other signals, the targets are still resolved in delay and Doppler, even in the close target scenario. This is due to the

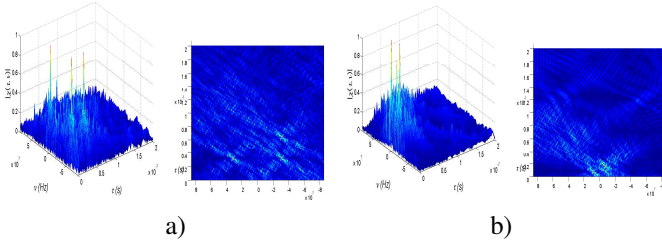


Fig. 11. CAF for a Doubly coded Costas signal: a) spaced targets scenario c) close targets scenario

low sidelobe level properties of those signals and the better Doppler resolution achieved due to the higher signal duration. However, this is still not sufficient for a real life application where the Doppler resolution must be lower. It could be improved considering a train of identical pulses that narrow the Doppler width according to novel train signal duration. The cross-ambiguity detection could be inefficient in the case of very low SNR multi-target scenario.

IV. EXPERIMENTAL RESULTS

In this part, we propose to show some experimentation based on the above signals. This helps to evaluate waveforms characteristics and performances in a real environment. The test bench is shown in Fig 12. The transmitted signal is centered around a carrier frequency $f_c = 2GHz$: $u_{RF}(t) = \Re(u(t)) \cos(2\pi f_c t) - \Im(u(t)) \sin(2\pi f_c t)$. At the receiver side, we perform an I/Q detection in order to reveal the in-phase and quadrature components and hence reconstitute the complex envelope $u(t) = \Re(u(t)) + i\Im(u(t))$. The CAF is then calculated between transmitted and received signal after reflection from a metal plate of $1m^2$. Here, since a static target is considered a detection with a correlator (zero-Doppler cut of cross-ambiguity function) could be sufficient. Hence, we also considered the cross-correlation CCF between transmitted and received signals. Results are shown in Fig 13 and Fig 14, when the signals shown in Table I are transmitted.

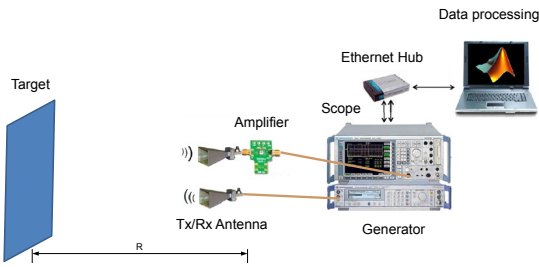


Fig. 12. Radar test bench description

We note that theoretical ACF and practical CCF are very similar. Indeed, the hardware effect, specially, the antenna differentiation, is not much visible and the CCF is preserved and produce a spike on the correct delay corresponding to the distance between the antenna and the target. The CAF's also show a centered spike in the correct delay and Doppler $(\tau, \nu) \approx (15.95ns, 0)$. Also, returns from the several signals are likely similar in the vicinity of the main lobe. This is due to surrounding environment and antenna leaks. Several

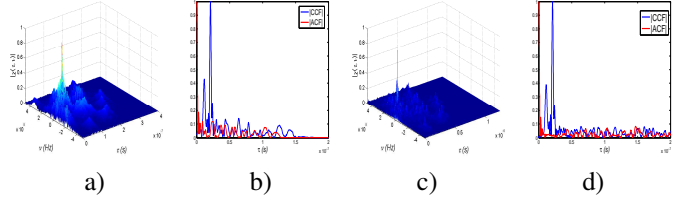


Fig. 13. a) CAF for a standard Costas signal, b) ACF and CCF for a standard Costas signal, c) CAF for a Costas-Hequi signal, d) ACF and CCF for a Costas-Hequi signal

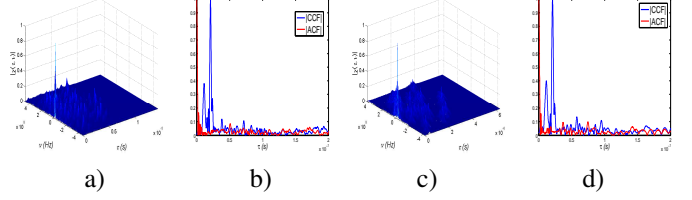


Fig. 14. a) CAF for a Costas-P4 signal, b) ACF and CCF for a Costas-P4 signal, c) CAF for a Doubly coded Costas signal, d) ACF and CCF for a Doubly coded Costas signal

experimentations must be done, considering moving targets also, in order to better evaluate performances and estimation accuracy.

V. CONCLUSION

In this paper, a detection scheme based on cross-ambiguity calculation is proposed. First, waveforms based on modified Costas codes are synthesized. A study of cross-ambiguity function properties on such waveforms is then proposed. Performances in presence of noise and multiple targets are evaluated. It was seen that proposed signals offer more robustness to noise and multiple targets because of the low sidelobes level. Finally, some experimentation results has been shown in order to validate the waveforms and evaluate their performances in a real-life scenario. This work should be extended to the evaluation of performances in terms of Delay and Doppler estimations. Furthermore, we must focus on more sophisticated scenarios in experimentation that help understand the radar environment constraints.

REFERENCES

- [1] M. Skolnik, *Radar Handbook, Third Edition*. McGraw-Hill Education, 2008.
- [2] N. Levanon and E. Mozeson, *Radar signals*. John Wiley and Sons, Inc, 2004.
- [3] J. Costas, "A study of a class of detection waveforms having nearly ideal range-doppler ambiguity properties," *Proceedings of the IEEE*, vol. 72, no. 8, pp. 996–1009, 1984.
- [4] N. Levanon and E. Mozeson, "Modified costas signal," *Aerospace and Electronic Systems, IEEE Transactions on*, vol. 40, no. 3, pp. 946–953, 2004.
- [5] N. Touati, C. Tatkeu, T. Chonavel, and A. Rivenq, "Phase coded costas signals for ambiguity function improvement and grating lobes suppression," in *Vehicular Technology Conference (VTC Fall), 2013 IEEE 78th*, 2013, pp. 1–5.
- [6] —, "Doubly coded costas signals for grating lobes mitigation," in *Personal Indoor and Mobile Radio Communications (PIMRC), 2013 IEEE 24th International Symposium on*, Sept 2013, pp. 481–485.